Impact of Interfering Bluetooth Piconets on a Collocated p-Persistent CSMA-Based WLAN

Imran Ashraf, *Member, IEEE*, Konstantinos Voulgaris, *Member, IEEE*, Athanasios Gkelias, *Member, IEEE*, Mischa Dohler, *Senior Member, IEEE*, and A. Hamid Aghvami, *Fellow, IEEE*

***Abstract*—In this paper, the effect of cochanneled Bluetooth (BT) piconets on a carrier-sense multiple-access (CSMA)-based wireless local area network (WLAN) is investigated. Specifically, the p-persistent CSMA protocol is considered for WLANs, and the probability of error of a WLAN packet is calculated in the presence of interfering BT packets of different lengths and variable piconet traffic loads and as a function of the BT's frequency-hopping guard time. The probability derivation is then used in conjunction with the p-persistent CSMA throughput and delay formulations to examine its net performance in the presence of BT interference. Simulations have been used to corroborate the analytical results, which indicate that the presence of just one fully loaded interfering BT piconet reduces the peak CSMA throughput by 42%. Furthermore, we show that under fully loaded BT traffic conditions, the effect of more shorter BT packet transmissions on the CSMA delay performance can outweigh the interference impact of a higher number of BT piconets with longer packet transmissions.**

***Index Terms*—Bluetooth (BT), carrier-sense multiple access (CSMA), interference, packet radio networks (PRNs), performance evaluation.**

I. Introduction and Problem Statement

THE demand for packet data services in conjunction with wireless mobility is experiencing a gradual increase. One of the offsprings of this "mobility and data services" union is the emergence of different packet radio technologies concurrently operating in unlicensed frequency bands [1]. This ignites the core issue of mutual interference in collocated packet radio networks (PRNs): a research concern that has rigorously been studied in the literature [2]–[7]. The existing research indicates that the mutual interference issue needs to comprehensively be addressed before simultaneously operating PRNs could optimally and efficiently be used together. As an example, the coexistence issue of Bluetooth (BT) and IEEE 802.11 wireless local area networks (WLANs) in the 2.4-GHz industrial, scientific, and medical (ISM) band has garnered significant interest from the research community, ranging from concrete interference characterization to advanced interference-mitigation solutions [8]–[13].

The coexistence of PRNs and the associated interference characterization pose challenging research problems from different perspectives. First, the choice of a performance evaluation method (simulation, analytical, or empirical) to study the interference in collocated PRNs is partially dependent on the similarities between the PRN protocols and the associated network characteristics (topology, transmission power, modulation schemes, packet structures, application characteristics, etc.). Generally, the complexity of performance evaluation for such environments increases when PRNs of heterogeneous radio characteristics are present, which makes computer-simulation techniques a preferred methodology. Analytical treatments, however, can readily provide first-order performance approximations in interference-affected scenarios but are more difficult to formulate when incorporating a diverse range of parameters in closed form [14], [15].

There are further interesting issues to consider within the wireless networks coexistence domain. For instance, if we assume a case of two mutually interfering PRNs located at some distance from each other and comparable channel gains, the network with low transmission power values generally experiences more interference from the interferer network with relatively higher transmit power [16]. This happens because high-energy interfering signals exhibit extremely low signal-to-interference-plus-noise ratio values at the desired receiver and, in effect, render the capture of the desired packets impossible. As an example, by considering the interference scenario of a BT piconet and an IEEE 802.11b WLAN and assuming fully loaded conditions in both networks, the BT piconet will suffer substantially more due to the high transmission power of WLAN, i.e., 100 mW compared with 1 mW of BT [17]. However, an increased population of low-powered BT personal area networks (PANs) can generate substantial interference. This is further augmented by the fact that BT is primarily intended to be used in the PAN domain, and there is a high possibility of more than one BT piconet operating in a single WLAN vicinity. A high density of BT devices [using frequency-hopping spread spectrum (FHSS)] results in an increased usage of the ISM

Manuscript received March 12, 2008; revised September 4, 2008 and July 9, 2009. First published July 21, 2009; current version published November 11, 2009. The work of I. Ashraf was supported in part by the Mobile-VCE Core 3 research program. The work of M. Dohler was supported in part by the Spanish government under Grant Torres Quevedo PTQ-08-01-06440 and in part by the Catalan government under Grant 2009 SGR 1046.

I. Ashraf is with the Autonomous Networks and Systems Research, Bell Laboratories, Alcatel-Lucent, SN5 7DJ Swindon, U.K. (e-mail: iashraf@alcatel-lucent.com).

K. Voulgaris is with Ofcom, SE1 9HA London, U.K. (e-mail: kostas.voulgaris@ofcom.org.uk).

A. Gkelias is with the Department of Electrical and Electronic Engineering, Imperial College London, SW7 2AZ London, U.K. (e-mail: a.gkelias@imperial.ac.uk).

M. Dohler is with CTTC, Parc Mediterrani de la Tecnologia, 08860 Castelldefels, Spain (e-mail: mischa.dohler@cttc.es).

A. H. Aghvami is with the Centre for Telecommunications Research, King's College London, WC2R 2LS London, U.K. (e-mail: hamid.aghvami@kcl.ac.uk).

Color versions of one or more of the figures in this paper are available online at http://ieeexplore.ieee.org.

Digital Object Identifier 10.1109/TVT.2009.2027811

0018-9545/$26.00 © 2009 IEEE

band and thus causes a very high probability of frequency overlapping between the two networks. For instance, the occupied bandwidth for IEEE 802.11b direct-sequence spread-spectrum (DSSS)-based WLAN is 22 MHz, and by considering uniform hopping of a single BT piconet in the 79 available channels (1 MHz wide each), the probability that the BT *does not* hop on to the WLAN channel is $(1-22/79) = 57/79 = 0.72152$. The presence of just one more independently operating BT piconet reduces this probability to $(57/79)^2 = 0.52059$: a reduction in the probability of no frequency overlapping by a factor of approximately 28%.

Apart from the number of collocated devices, the traffic patterns of interfering networks can also cause variable interference effects. The traffic models are in turn dependent on the type of application used. Low-cost and low-powered wireless PANs, akin to BT piconets, offer a diverse range of services and applications to the end user, such as wireless earphones, keyboards, and short-range time-bounded information exchange. Such diversity in the nature of applications draws an interesting effect on the mutual interference issue. Applications that require continuous transmission of packets, such as real-time data communications supported by synchronous connection-oriented (SCO) links in BT, may cause large instantaneous interference to an intended receiver. On the other hand, applications carrying bursty traffic, such as that handled by asynchronous connectionless (ACL) links, may appear less harmful. However, an interesting observation is that the packets transmitted over SCO links in BT are never retransmitted. ACL links, on the contrary, may request retransmissions of corrupted packets, which could result in significant traffic generation (high interference) in highly populated spectrum conditions. Therefore, the nature of usage and the range of applications belonging to an interfering network can greatly influence a successful packet reception in the victim network.

II. Related Work and Our Contributions

Of the various radio access technologies, the mutual interference between BT and IEEE-802.11-based WLANs in the 2.4-GHz ISM band has attracted the greatest attention. The foremost reason for this research direction is the popularity of the two PRNs, which are being used and extensively deployed together (in millions) in a large number of countries around the world. In the following, we review the existing literature on the mutual interference scenario of BT and IEEE-802.11-based WLANs.

Generally, the research presented in [8], [10], and [18]–[24] mostly relies on simulation frameworks or measured experimental results to study the coexistence between the two wireless systems. Punnoose *et al.* [8] rely on measurement results to evaluate the performance of an interfered BT link. In [10], the effect of mutual interference on both BT and IEEE 802.11b links is investigated, and measurements are also taken to validate the simulation results. In [18], simulation results are presented at bit level, highlighting the effect of IEEE 802.11b on BT. The authors present results from a coexistence testbed in [19] and [20], where the main aim is to validate the simulation models using measurements from a real-life testbed. The BT packet error probability due to IEEE 802.11b interference is given in [21] using a basic Physical (PHY) layer analytical model. The work reported in [22] and [23] presents a simulation environment for modeling IEEE 802.11 and BT interference based on detailed PHY layer and medium access control (MAC) layer models. Other papers, e.g., [11] and [25], propose coexistence mechanisms using different traffic-scheduling techniques that mitigate the interference between BT and IEEE 802.11b WLANs.

Analytical treatments on the BT-802.11 interference issue have been well presented in [3], [12]–[14], and [26]. In [3], Howitt gives a closed-form solution for the probability of packet collision using a lognormal shadowing radio propagation model and considering adjacent band interference. However, only single-slot BT packets are considered in the analysis. The same author in [12] analytically examines the impact that an 802.11b network has on BT performance. The approach is based on empirical results to develop the analytical model under varying interference scenarios. The key assumptions in the analysis are single-slot BT packets and the consideration of a mean delay period between 802.11b packet transmissions. An integrated coexistence analytical model is given in [13], entailing various PHY and MAC aspects. However, the authors focus on a more combined approach and do not incorporate the probability of time coincidence between overlapping packets and the BT frequency-hopping guard time, which have a serious effect on the packet error rate. In [9], Ashraf *et al.* study the interference effect of a p-persistent carrier-sense multiple-access/collision-avoidance (CSMA/CA) protocol on a BT piconet's throughput using a detailed CSMA model; but the opposite scenario of BT's interference on CSMA is not given any attention. More recently, in [14], Stranne *et al.* have proposed an energy-based interference analysis of heterogeneous PRNs and explored BT and IEEE 802.11b throughput behavior as an example. The work in [14] takes into account the basic path-loss model and adjacent channel interference; however, it is assumed that no intrasystem interference exists. From the CSMA-based WLAN point of view, this assumption implies that the packets are not lost due to channel contention between the CSMA users, which does not hold true particularly in high-traffic conditions.

Our Contributions: The emphasis of this paper resides on the performance evaluation of a p-persistent CSMA protocol under the effect of cochannel interference. The p-persistent protocol involves a probabilistic mechanism to avert collisions between the contending CSMA nodes and can closely model the behavior of the IEEE 802.11 MAC protocol (see [27]–[29] for detailed discussions), which makes it a justified choice for our study. Furthermore, models developed for the p-persistent case can greatly aid in the analysis of more complex CSMA flavors. The p-persistent case presents the baseline for the CSMA family of MAC protocols. Enhancements to the model include the exchange of control information, such as request-to-send/clear-to-send packets, to improve system performance [30]. However, the analytical modeling generally entails the treatment of simpler CSMA models first before incorporating the characteristics of more complex models.

The main contributions of this paper are summarized as follows.

1) First, and as reflected from Section II, the related work in the literature fails to address a thorough examination of the CSMA MAC in the presence of interference from a collocated PRN. CSMA parameters had partially been integrated in the already existing analyses, either by assuming averaged quantities or by quantifying values from empirical results of specific scenarios. Our research stands apart from this prior work in that it explicitly studies the CSMA performance by developing a comprehensive model for its channel throughput and end-to-end delay characteristics in the presence of interfering BT piconets.

   From another standpoint, our work delivers insights in the performance of higher layers in interference-affected PRNs. It is important to understand this phenomenon as packet collisions at the PHY layer may lead to poor scheduling patterns at the MAC layer, which can subsequently limit the interference-mitigation opportunities at the transport layer [31].
2) Second, we formulate the probability of success for a WLAN[1] packet in the presence of both internal (from contending WLAN users) and external interference (from BT piconets). Specifically, we derive it as a function of WLAN and BT offered traffic loads, WLAN and BT packet lengths, BT frequency-hopping guard time, and the number of interfering BT piconets. Although our work adopts certain PHY layer specifications from IEEE 802.11b and BT to facilitate the plotting of results, the rationale behind the model is its generic nature, which makes it adaptable to parameter settings from PRNs with similar characteristics.

It is important to mention that the analysis presented hereafter does not include transmit power levels and the associated channel modeling. Incorporating the channel model delivers a more realistic behavior of the system and expectedly increases the complexity of the analysis. However, in the context of heterogeneous PRNs, it is always of interest (and generally difficult) to develop models that can entail diverse characteristics of the involved networks. Our model comprehensively characterizes the CSMA's behavior in the presence of multiple independently operating BT piconets in dependency of a number of variable parameters belonging to both WLAN and BT. As such, in the absence of the capture model, it presents the lower bounds on CSMA performance.

The rest of this paper is organized as follows: The underlying coexistence model and its analysis is presented in Section III, wherein we formulate the probability of success of a CSMA packet in the presence of BT interference, i.e., P_{BT}^{S}. It is then used in conjunction with the p-persistent CSMA channel access model to derive its throughput and delay performance in the presence of BT interference in Sections IV and V, respectively, along with the corresponding numerical results.

[1]As our WLAN is based on CSMA MAC, we interchangeably use the terms "CSMA" and "WLAN."

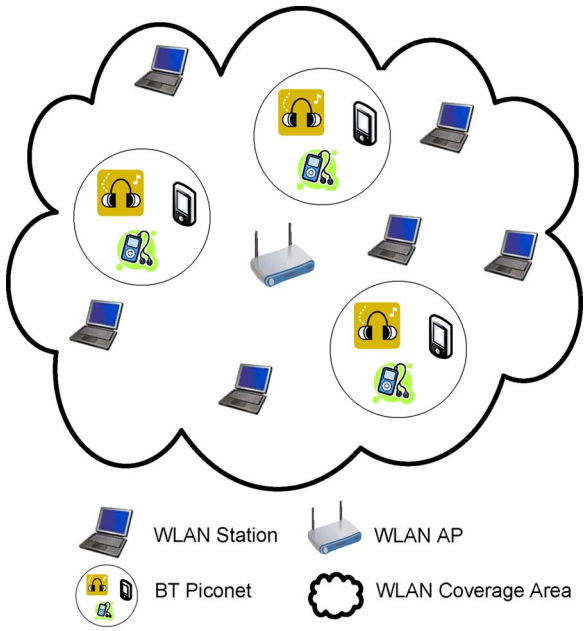

Fig. 1. Network topology of spatially overlapped BT piconets and WLAN stations within a WLAN's coverage area. The WLAN's topology could be infrastructure based (as shown) or based on the ad hoc mode.

Finally, conclusions vis-a-vis the research in this paper are drawn in Section VI.

III. Coexistence Analysis

A. Interference Model

The interference model is shown in Fig. 1, where a number of BT piconets exist within the radio coverage area of a WLAN. A slotted p-persistent CSMA model is adopted for WLAN stations contending for the channel toward a common receiver, be it in the centralized mode toward an AP or in the ad hoc mode toward another WLAN station. The WLAN consists of M number of users and operates over a varying range of offered load conditions. To portray a relatively worst-case scenario, we assume that the WLAN employs a clear channel assessment (CCA) procedure that is only able to sense other WLAN signals, i.e., any interfering BT signal is not interpreted as occupying the channel. Practically, this is a valid assumption, particularly if CCA Modes 2, 3, 4, or 5 are used from the IEEE 802.11b standard [32], [33]. Furthermore, it is assumed that all coexisting networks independently operate, and no means of coordination exists between them. This is typically the operational scenario of coexistence between multiple PRNs, particularly those that are heterogeneous in nature.

The number of collocated BT piconets is denoted by N, and the same traffic load is considered in each BT piconet to make the analysis tractable. BT employs FHSS, and we assume that each BT piconet adopts a uniformly distributed hopping pattern over the 79 available frequency channels (1 MHz wide each). This assumption is generally used to simplify the analysis [34]–[36]; however, tighter bounds on the packet error rate can be achieved by modeling short-term frequency dependencies in the BT hop sequence [37].

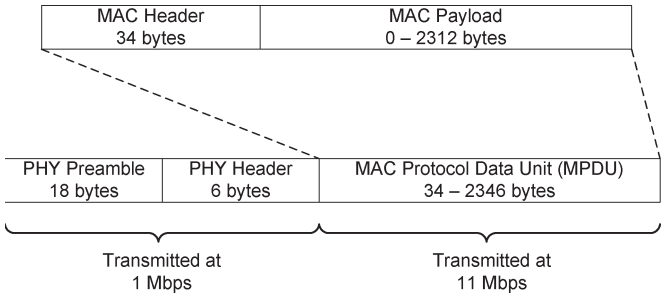

Fig. 2. Data frame format from the IEEE 802.11b specifications [33].

Furthermore, we have not included power control, i.e., the ability of the terminals to control their transmit and hence generated interference power, nor have we incorporated capture effects, i.e., the ability to receive a packet although interfered because the received power is sufficiently high compared with the aggregate interference power. This clearly constitutes a worst-case scenario and suffices to concentrate on the core of this paper, which is the interplay of a large number of integrated BT and WLAN system parameters. Note that the inclusion of both power control and capture effect into our analysis is possible but unnecessarily clutters the exposure.

Definition: The WLAN packet is corrupted if two or more users within the WLAN simultaneously transmit or if a single WLAN packet transmission is overlapped in both time and frequency by one or more BT packets from any of the N collocated piconets.

We represent the probability of success (no time and frequency overlapping) of a WLAN packet in the presence of a single BT piconet by $P_{\rm BT}^S$. Next, we proceed to calculate $P_{\rm BT}^S$ and use it to evaluate the throughput and delay of CSMA/CA in the presence of BT interference.

B. Interference Analysis

Our interference analysis is based on the approach used in [4] and [26]. Specifically, we use the following notations in the derivation of $PS_{\rm BT}^2$ (see also Fig. 3):

1) T_W: length (in time units) of the PHY layer WLAN packet. To consider realistic values for packet lengths and associated data rates, we follow the data frame format specifications in [33] and further exemplified in Fig. 2. As shown, the size of the PHY layer packet varies from 58 to 2370 B. Furthermore, the entire PHY layer Header and Preamble of 24 B are transmitted using the basic data rate of 1 Mb/s, which takes 192 μs. As an example, for a PHY layer WLAN packet size of 1400 B, the MAC protocol data unit (MPDU) consists of $1400-24=1376$ B, which, at a transmission rate of 11 Mb/s, requires $((1376\times 8)/(11\times 10^6))=1000.73$ μs. The total transmission time of the PHY layer WLAN packet thus equates to $T_W = 192 + 1000.73 \approx 1193$ μs;
2) $T_{\rm BT}$: length of the BT slot, i.e., $T_{\rm BT} = 625$ μs [38];
3) $T_{{\rm BT},i}$: length of an i-slot BT packet, $i = 1, 3$, and 5, given as $T_{{\rm BT},i} = i \times T_{\rm BT}$;
4) N_W: number of BT slots (of length $T_{\rm BT}$) partially or fully occupied by the WLAN packet of length T_W, i.e., $N_W = \lceil T_W/T_{\rm BT} \rceil$, where $\lceil\cdot\rceil$ represents the ceil function;

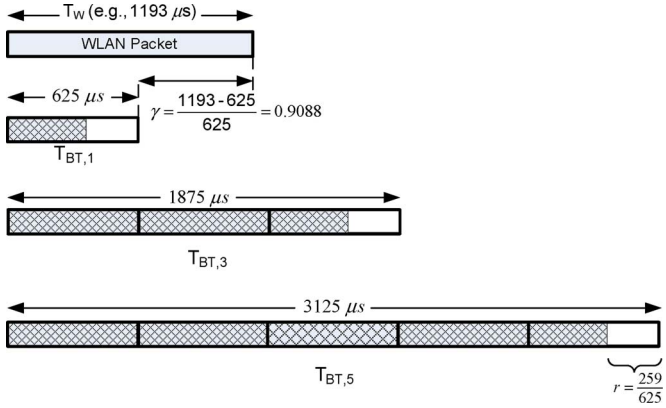

Fig. 3. Graphical description for the set of notations used in the analysis.

5) r: frequency-hopping guard time in BT packets normalized to the BT slot length. According to the BT specifications [38], the value of r is equal to 259/625, 253/625, and 255/625 for one-, three-, and five-slot packets, respectively. Without loss of generality, we assume a single value of r, i.e., $r = 259/625 = 0.4144$ [4];
6) γ: If the WLAN packet is not an exact multiple of the BT slot length, then γ represents the residual part of the WLAN packet normalized to the BT slot length, i.e., $\gamma = T_W - (N_W - 1)T_{\rm BT}/T_{\rm BT}$. For example, for $T_W = 1193$ μs, $N_W = 2$, and $\gamma = 0.9088$.

Let us consider a single coexisting BT piconet Y, which is the unique source of external interference to ongoing packet transmissions within the WLAN. The BT nodes in piconet Y can transmit either one-, three-, or five-slot (DH1, DH3, or DH5) packet. For multislot BT packets, we associate arrival probabilities to each of the constituent slots to cater to the fact that the transmissions of WLAN and BT packets are completely unsynchronized. This means that the WLAN packet can start at any instance during an ongoing BT transmission (see Fig. 6), e.g., it could start during the second slot of a DH3 transmission or the fourth slot of a DH5 packet. We denote the arrival probabilities for each of the one-, three-, and five-slot packets as ρ_1, ρ_3, and ρ_5, respectively. The BT piconet's time used in activities other than the data traffic or the idle time is modeled by assuming a single-slot empty packet with probability ρ_0 such that $\rho_0 = 1 - (\rho_1 + \rho_3 + \rho_5)$. Letting ϕ be the set defined for different BT packet types such that $\phi = \{0, 1, 3, 5\}$, then the arrival probabilities of the constituent slots for each of the packet types can be represented by $\rho_{i,j}$, where $i \in \phi$, and $j \in [1, \max(1, i)]$. Here, the subscript i represents the BT packet type, and j denotes the position of the slot within the packet. Moreover, $(\rho_{0,1} = \rho_0)$, $(\rho_{1,1} = \rho_1)$, $(\rho_{3,1} = \rho_{3,2} = \rho_{3,3} = \rho_3/3)$, and $(\rho_{5,1} = \rho_{5,2} = \rho_{5,3} = \rho_{5,4} = \rho_{5,5} = \rho_5/5)$. We also define $\sigma_{i,j}$ to be the number of slots in an i-slot packet that follow the beginning of the slot position j such that $\sigma_{i,j} = 1$ for $i = 0$ and $\sigma_{i,j} = i - j + 1$ for $i > 0$. As an example, $\sigma_{0,1} = \sigma_{1,1} = 1, \sigma_{3,2} = 2$, and $\sigma_{5,3} = 3$.

Furthermore, considering that an ongoing WLAN packet transmission uses $\xi_W = 22$ MHz of the ISM band, the probability that piconet Y chooses a frequency from the

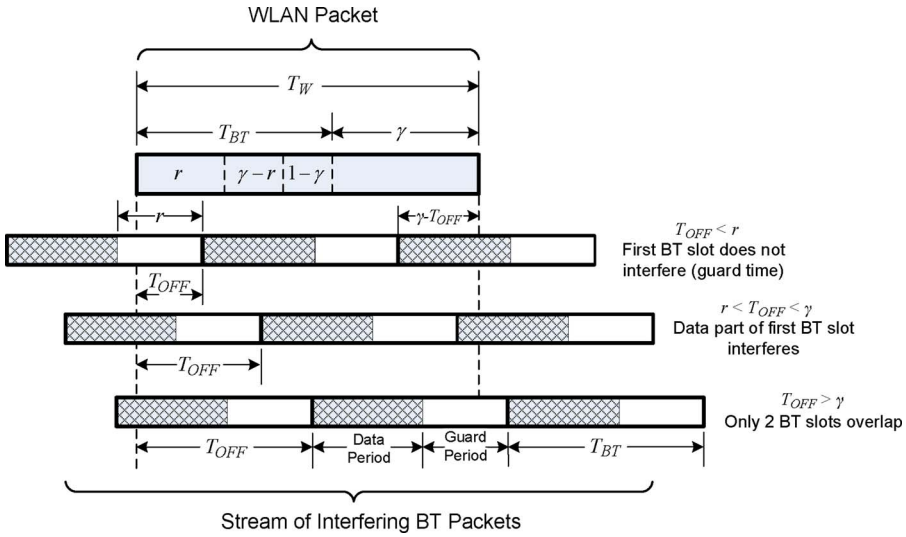

Fig. 4. Temporal overlapping of simultaneously transmitted WLAN and BT packets for the case ($T_W > T_{\mathrm{BT}}$) and ($r \leq \gamma$). Note that r and γ are normalized to T_{BT}.

79 available channels other than the 22 MHz is $P_0 = (1 - 22/79) = 57/79$. Given P_0 and the fact that two successive BT packets are transmitted on a different frequency, the probability for the next BT packet to use a frequency other than the 22 MHz used by WLAN is $\tilde{P}_0 = (1 - 22/78) = 56/78$.

To aid in the formulation of P_{BT}^S, let us consider the packet collision example shown in Fig. 4, which illustrates temporal overlapping patterns of the given WLAN packet and different BT slots. We note that the WLAN packet is successful if it survives the interference from the first interfering BT packet and all the subsequent packets. We formulate the success probability under the interference from the first BT packet and denote it by f, whereas the success probability under the interference caused by all later BT slots is denoted by β. The calculation of these probabilities is directly linked to the offset of the first occurring BT slot boundary from the start of the WLAN packet, which is expressed as T_{OFF} and follows a continuous uniform distribution such that $T_{\mathrm{OFF}} \in U(0, 1]$.

To explain the dependence of f on T_{OFF}, recall the frequency-hopping guard time r of a BT packet, during which there is no data transmission. If $T_{\mathrm{OFF}} \leq r$, and the first occurring BT slot is the last slot of a BT packet ($i = j$), then the overlapping portion of the interfering packet is empty and does not interfere with the WLAN packet. On the other hand, if $T_{\mathrm{OFF}} > r$, then the ongoing BT transmission interferes with the WLAN packet with probability P_0. We denote the WLAN's packet success probability in the former case by $\tilde{f}$ and in the latter by $\hat{f}$. The corresponding expressions are given as

$$\tilde{f}(i,j) = \begin{cases} 1, & \text{if } i = j \text{ or } i = 0 \\ P_0, & \text{otherwise} \end{cases} \tag{1}$$

$$\hat{f}(i,j) = \begin{cases} 1, & \text{if } i = 0 \\ P_0, & \text{otherwise.} \end{cases} \tag{2}$$

The derivation of β follows a different approach in that it uses a recursive formulation to identify how many BT packets (of any allowed size) can fit in a given number of BT slots and their corresponding probability of interfering with the WLAN packet. The formulation of β is given as follows for $m > 0$:

$$\begin{aligned} \beta(m) = & \frac{\rho_0}{\rho_0 + \rho_1 + \rho_3 + \rho_5} \cdot \beta(m - \sigma_{0,1}) \\ & + \frac{\rho_1}{\rho_0 + \rho_1 + \rho_3 + \rho_5} \cdot \tilde{P}_0 \cdot \beta(m - \sigma_{1,1}) \\ & + \frac{\rho_3}{\rho_0 + \rho_1 + \rho_3 + \rho_5} \cdot \tilde{P}_0 \cdot \beta(m - \sigma_{3,1}) \\ & + \frac{\rho_5}{\rho_0 + \rho_1 + \rho_3 + \rho_5} \cdot \tilde{P}_0 \cdot \beta(m - \sigma_{5,1}) \end{aligned} \tag{3}$$

where $\beta(m) = 1$ for $m \leq 0$. The offset duration T_{OFF} determines the total number of BT slots fully or partially overlapping with the WLAN packet, which is $N_W + 1$ if $T_{\mathrm{OFF}} < \gamma$, and N_W otherwise. The number of slots that needs to be considered for the calculation of β is that previously mentioned, less the remaining slots from the ongoing BT packet given by $\sigma_{i,j}$.

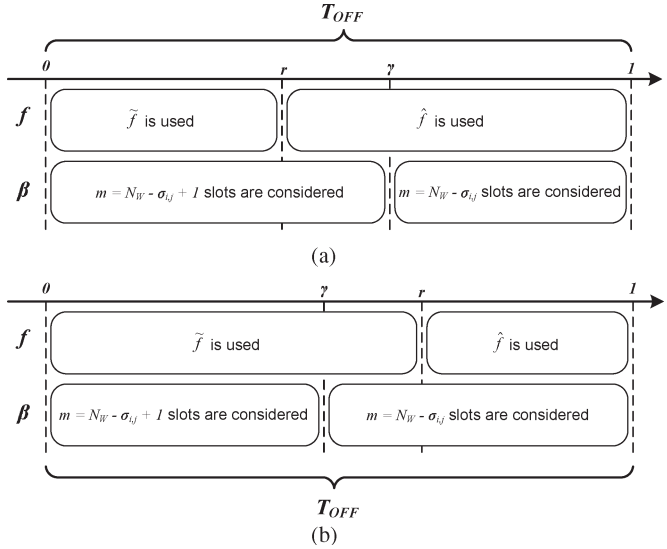

Fig. 5. Dependence of f and β on the length of T_{OFF} for (a) $r \leq \gamma$ and (b) $r > \gamma$.

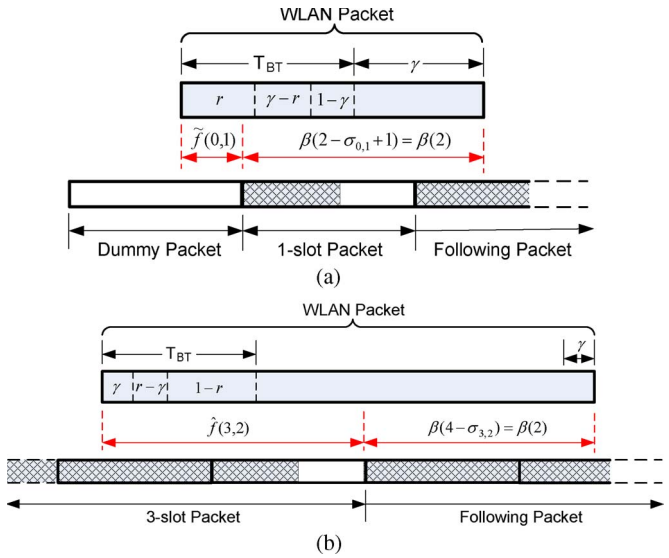

Fig. 6. Examples of success probability calculations for different WLAN packet lengths.

Summarizing the foregoing results and combining the dependencies of r and γ on T_{OFF}, we get Fig. 5(a) and (b) for both $(r \leq \gamma)$ and $(r > \gamma)$, respectively, which dictate the different parts of the P_{BT}^{S} formulation in (4), shown at the bottom of the page.

By including the arrival probabilities $\rho_{i,j}, i \in \phi$ and $j = 1, \ldots, \max(1, i)$ in (4), we consider that each of the BT slots can first overlap with the WLAN packet. The probability functions $\tilde{f}(i,j)$ and $\hat{f}(i,j)$ defined in (1) and (2) give the probability that the first packet of piconet Y does not interfere with the WLAN packet. The recursive function $\beta(m)$ takes into account the success of the remaining portion of the WLAN packet by including the possibility of occurrence of all BT packet types.

As an example, Fig. 6(a) illustrates the packet collisions between a WLAN packet and multiple BT packets transmitted from the piconet Y. We observe that the WLAN packet occupies two BT slot lengths, i.e., $N_W = 2$, and $\gamma > r$. The first interfering BT slot belongs to a dummy packet, which ends during the first r portion of the WLAN packet $(T_{\mathrm{OFF}} < r)$. Thus, the success probability of the first part of the WLAN packet (up until the end of dummy packet) becomes $\tilde{f}(0,1) = 1$. The success of the remaining portion of the WLAN packet is characterized by the probability function $\beta(2)$. The total success probability of the WLAN packet is thus given as $r \cdot \rho_{0,1} \cdot \tilde{f}(0,1) \cdot \beta(2)$. Fig. 6(b) shows another example, where $N_W = 4$, and $\gamma < r$.

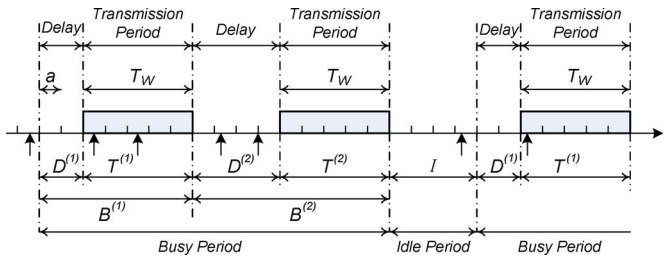

Fig. 7. Channel model for slotted p-persistent CSMA [39]. Small upward arrows indicate the generation of packets by users.

The first interfering slot from Y is the second slot of a DH3 packet, and it ends during the $(1 - r)$ portion of the WLAN packet $(T_{\mathrm{OFF}} > r)$. The success probability from the beginning of WLAN packet up until the end of the third slot of DH3 packet thus becomes $\hat{f}(3,2) = P_0$. For the remaining part, the success probability is equal to $\beta(2)$. The final success probability is therefore given as $(1 - r) \cdot \rho_{3,2} \cdot \tilde{f}(3,2) \cdot \beta(2)$.

Equation (4) gives the probability of success for a WLAN packet of length T_W in the presence of a single interfering piconet Y. In the presence of N independent and identically distributed (i.i.d.) BT piconets, the probability of both time and frequency overlapping is given as $P_{\mathrm{BT}}^{C} = 1 - (\frac{S}{\mathrm{BT}})^{N}$. Furthermore, (4) can easily be extended for any packet length distribution of the interfering FHSS system (apart from the one-slot, three-slot and five-slot BT packets considered here) by modifying the interfering packet type set ϕ and the corresponding arrival probabilities ρ_i and adjusting $\sigma_{i,j}$ to reflect new packet lengths.

IV. Carrier-Sense Multiple-Access/ Collision-Avoidance Throughput Performance

In this section, we derive the throughput of a slotted p-persistent CSMA in the presence of interference from N interfering BT piconets. As the throughput derivation is largely based on [39], we assume that the reader is well aware of the slotted p-persistent CSMA model presented therein. Therefore, we intentionally ignore rewriting all equations and only list the most relevant equations.

We start by recalling the Renewal-Theory-based slotted p-persistent CSMA channel model originally presented in [39] and shown in Fig. 7. In slotted CSMA, the time is slotted with slot size a, and all CSMA users are assumed to be synchronized to start transmission at slot boundaries. A slight difference in the model presented in this paper is the assumption of negligible

$$P_{\mathrm{BT}}^{S} = \begin{cases} \sum\limits_{i \in \phi} \sum\limits_{j=1}^{\max(1,i)} \Big\{ r \cdot \Big[\rho_{i,j} \cdot \tilde{f}(i,j) \cdot \beta(N_W - \sigma_{i,j} + 1) \Big] + (\gamma - r) \cdot \Big[\rho_{i,j} \cdot \hat{f}(i,j) \cdot \beta(N_W - \sigma_{i,j} + 1) \Big] \\ \qquad + (1 - \gamma) \cdot \Big[\rho_{i,j} \cdot \hat{f}(i,j) \cdot \beta(N_W - \sigma_{i,j}) \Big] \Big\}, & r \leq \gamma \\ \sum\limits_{i \in \phi} \sum\limits_{j=1}^{\max(1,i)} \Big\{ \gamma \cdot \Big[\rho_{i,j} \cdot \tilde{f}(i,j) \cdot \beta(N_W - \sigma_{i,j} + 1) \Big] + (r - \gamma) \cdot \Big[\rho_{i,j} \cdot \tilde{f}(i,j) \cdot \beta(N_W - \sigma_{i,j}) \Big] \\ \qquad + (1 - r) \cdot \Big[\rho_{i,j} \cdot \hat{f}(i,j) \cdot \beta(N_W - \sigma_{i,j}) \Big] \Big\}, & \text{otherwise} \end{cases} \tag{4}$$

signal propagation delay, which was assumed to be of length a in [39]. To analyze the throughput, we use the same set of notations as explained in [39]. For ease of use in this section, we recall some notations:

1) M: number of CSMA users[2] contending for the wireless medium;
2) a: slot length (in time units) for the slotted CSMA model. From IEEE 802.11b [33], it is defined as a SlotTime with a value of 20 μs. It is different from the channel partitioning (of length 625 μs) in the BT PHY link;
3) $T_{W,N}$: number of slots occupied by the WLAN packet of length T_W, i.e., $T_{W,N} = \lceil T_W/a \rceil$, where the ceil function $\lceil \cdot \rceil$ is used to include partially occupied slots;
4) g: probability of a terminal to generate a packet during one slot length a; thereby referred to as the *ready* terminal. The value of g is considered to be the same for all users;
5) p: probability of a ready terminal to transmit a packet. The value of p is also assumed to be the same for all users;
6) N_0: number of CSMA users that are ready at the end of a packet-accumulation time (X);
7) D: delay in between consecutive transmissions (successful or not) due to the users contending for the channel;
8) N_k: number of CSMA users that are ready until the kth slot of the delay period D;
9) B: channel busy period (in time units) in which there is a transmission (successful or not) or at least one of the M terminals has a packet ready to be transmitted. As shown in Fig. 7, the channel busy period is divided into several sub(busy)periods such that jth sub(busy)period $B^{(j)}$ consists of transmission delay $D^{(j)}$ followed by transmission time $T^{(j)}$;
10) I: channel idle period in which no CSMA packets are awaiting transmission. The idle period starts if no packets are generated in the packet accumulation time of the last sub(busy)period. The expected value is derived as $\bar{I} = a/(1-(1-g)^M)$;
11) U: time spent for successful transmissions in a busy period B;
12) J: total number of sub(busy)periods in a busy period B. Its average is given by $\overline{J} = 1/(1-g)^{(T_{W,N})M}$;
13) superscript numbering for the channel states, such as $D^{(1)}$ or $U^{(2)}$, refers to the value in the corresponding sub(busy)period. For instance, $D^{(1)}$ refers to the delay in the first sub(busy)period, whereas $U^{(2)}$ refers to the useful transmission time in the second sub(busy)period. As explained in [39], the first sub(busy)period starts after a packet accumulation time of $X = 1$ slot, whereas the rest of the sub(busy)periods are i.i.d. and have a packet accumulation time of $X = T_{W,N}$ slots.

Based on the foregoing definitions and in the absence of any external interfering source, the CSMA channel throughput S is given by the ratio $\overline{U}/\overline{B} + \overline{I}$ [39]. In the presence of interference from N i.i.d. BT piconets and keeping in mind the definition of packet error, the CSMA throughput is expressed as

$$S = \frac{\overline{U}}{\overline{B}+\overline{I}} \cdot (1 - P_{\mathrm{BT}}^{C}) = \frac{\overline{U}}{\overline{B}+\overline{I}} \cdot (P_{\mathrm{BT}}^{S})^{N} \tag{5}$$

where the average useful $(\overline{U})$, busy $(\overline{B})$, and idle $(\overline{I})$ times for a slotted p-persistent CSMA have been calculated in [39]. For the difference in assumption of negligible signal propagation delay, these are formulated as under

$$\begin{aligned}\overline{U} = {} & \frac{pMT_W}{(1-g)^{(T_{W,N})M}} \sum_{k=0}^{\infty} \Bigg\{ (1-p)^k - (1-g)^{(T_{W,N})} \\ & \cdot \left[\frac{(p(1-p)^k - g(1-g)^k}{p-g} \right] \Bigg\} \\ & \cdot \Bigg\{ (1-p)^{k+1} - p(1-g)^{(T_{W,N})} \\ & \times \left[\frac{(1-p)^{k+1} - (1-g)^{k+1}}{p-g} \right] \Bigg\}^{M-1}. \end{aligned} \tag{6}$$

$$\begin{aligned}\overline{B}+\overline{I} = {} & \overline{D^{(1)}} + T_W + \left[(1-g)^{(T_{W,N})M} - 1 \right] \\ & \cdot \left(\overline{D^{(2)}} + T_W \right) + \overline{I} \\ = {} & \frac{T_W}{(1-g)^{(T_{W,N})M}} + \frac{a}{(1-g)^{(T_{W,N})M}} \\ & \cdot \sum_{k=1}^{\infty} \Bigg\{ (1-p)^k - p(1-g)^{(T_{W,N})} \\ & \cdot \left[\frac{(1-p)^k - (1-g)^k}{p-g} \right] \Bigg\}^{M}. \end{aligned} \tag{7}$$

Note that (5) explicitly assumes that each WLAN packet is independently interfered with BT transmissions, i.e., the distribution of interfering BT packets as seen by each WLAN packet is i.i.d. The assumption is adopted to make the analysis tractable; in reality, however, the distribution of the interfering BT packets on successive WLAN packets is not totally independent and depends on factors, such as the channel access delays in between CSMA transmissions and the relative packet lengths of the WLAN and BT packets. Such dependencies are extremely difficult to include in the analytical model, and we show in the next section that our assumption generates a marginal deviation from the simulation results.

A. Numerical Results

Numerical results for the derived CSMA/CA throughput are presented in this section. We performed Monte Carlo simulations in C++ to verify the accuracy of the model. Computer simulations follow the same network setup as described in the aforementioned analytical model. Table I contains definitions and values for the parameters used throughout this paper. For CSMA/CA, the packet transmission probability is set to $p = 0.03$. Assuming a PHY layer data rate of 11 Mb/s (see Fig. 2), we consider three packet sizes for WLAN, i.e., 500 B ($T_W = 538$ μs), 1400 B ($T_W = 1193$ μs), and 2300 B ($T_W = 1847$ μs). Where the effect of different WLAN packet sizes is not considered in the plots, the medium-sized PHY layer

[2]We interchangeably use the terms "user," "node," and "terminal."

TABLE I
PARAMETER DEFINITIONS AND VALUES

	Parameter	Definition	Value or Range
Bluetooth Parameters	N	Number of Interfering BT piconets.	1 to 20.
	T_{BT}	BT slot length.	625 μs.
	$T_{BT,i}$	i-slot BT packet length, where $i = 1$ for the dummy packet. $T_{BT,i} = i \times T_{BT}$.	$T_{BT,1} = 625$ μs, $T_{BT,3} = 1875$ μs, and $T_{BT,5} = 3125$ μs.
	r	Normalized BT frequency hopping guard time.	$r = \frac{259}{625} = 0.4144$.
	ρ_i	Arrival probability of different BT packet types, where $i \in \phi = \{0, 1, 3, 5\}$.	0 to 1, such that $\rho_0 + \rho_1 + \rho_3 + \rho_5 = 1$.
	$\rho_{i,j}$	Arrival probability of slot number j in a BT packet of type i, where $i \in \phi = \{0, 1, 3, 5\}$ and $j \in [1, \max(1, i)]$.	$\rho_{0,1} = \rho_0$; $\rho_{1,1} = \rho_1$; $\rho_{3,1} = \rho_{3,2} = \rho_{3,3} = \frac{\rho_3}{3}$; $\rho_{5,1} = \rho_{5,2} = \rho_{5,3} = \rho_{5,4} = \rho_{5,5} = \frac{\rho_5}{5}$.
	$\sigma_{i,j}$	The number of slots in BT packet of type i that follow the beginning of the slot position j. $\sigma_{i,j} = 1$ for $i = 0$, and $\sigma_{i,j} = i - j + 1$ for $i > 0$.	$\sigma_{0,1} = 1$; $\sigma_{1,1} = 1$; $\sigma_{3,1} = 3$, $\sigma_{3,2} = 2$, $\sigma_{3,3} = 1$; $\sigma_{5,1} = 5$, $\sigma_{5,2} = 4$, $\sigma_{5,3} = 3$, $\sigma_{5,4} = 2$, $\sigma_{5,5} = 1$.
WLAN Parameters	M	Number of WLAN users.	1, 5, 15, 25, and 50.
	ξ_W	Transmission Bandwidth.	22 MHz.
	a	aSlotTime [33].	20 μs.
	g	The probability of WLAN user to generate a packet.	0 to 1.
	p	The probability of WLAN user to transmit a packet.	0.03.
	G	Offered traffic load, $G = gM/a$.	0.1 to 300 Erlang.
	T_{OH}	PHY and MAC headers transmission time.	216.73 μs.
	T_W	Total PHY layer WLAN packet length.	538 μs, 1193 μs, and 1847 μs.
	N_W	Number of BT slots partially or fully occupied by a WLAN packet of length T_W, $N_W = \lceil \frac{T_W}{T_{BT}} \rceil$.	$N_W = 1$ for $T_W = 538$ μs, $N_W = 2$ for $T_W = 1193$ μs, and $N_W = 3$ for $T_W = 1847$ μs.
	γ	If the WLAN packet is not an exact multiple of the BT slot length, γ is the residual part normalized to the BT slot length, $\gamma = \frac{T_W - (N_W - 1)T_{BT}}{T_{BT}}$.	$\gamma = 0.8608$ for $T_W = 538$ μs, $\gamma = 0.9088$ for $T_W = 1193$ μs, and $\gamma = 0.9552$ for $T_W = 1847$ μs.

packet length of $T_W = 1193$ μs is used. For BT, unless stated otherwise, equal arrival probabilities for each of the three packet (DH1/3/5) types are assumed. Furthermore, to obtain the numerical throughput curves, up to 1000 terms have been used in the infinite summations of (6) and (7), after which, the series converges for any value of g.

Fig. 8 plots the throughput degradation in CSMA as a function of the number of collocated BT piconets N. A fixed value for the CSMA's packet generation probability is considered, which is set to $g = 0.1$. The throughput curves are plotted for different number of contending WLAN users, i.e., $M = 5, 25$, and 50.

In Fig. 8(a), which plots throughput values for 100% traffic $(\rho_0 = 0)$ in each BT piconet, we observe that the normalized CSMA channel throughput S decays with an increasing number of BT piconets and reduces to approximately zero for $N = 10$. Even for a saturated BT traffic load, due to BT frequency hopping, there will always be a number of successfully transmitted WLAN packets for a small number of interfering piconets. However, this probability of success decreases as the number of BT piconets increases. Note that due to independent frequency-hopping patterns in individual BT piconets, an increase in the value of N lowers the probability that none of the BT piconets will hop in the frequency band used by the WLAN network. Nevertheless, for large values of N, there is a small probability for a successful WLAN packet transmission that approaches zero as N grows even larger.

In addition, Fig. 8(a) conveys that one collocated BT piconet can create more degradation to the WLAN channel throughput than the addition of a considerable number of WLAN terminals. For instance, in a WLAN network with five terminals and no external BT interference, the addition of 20 more WLAN terminals reduces the normalized channel throughput by approximately 21% (S is reduced from 0.85 to 0.67), whereas the addition of only one BT piconet to the system degrades the CSMA channel throughput by approximately 42% (S is reduced from 0.85 to 0.49). This is due to uncoordinated packet transmissions between the two heterogeneous networks. A possible remedy, which is akin to adaptive frequency hopping (AFH) [40], can be employed by the BT piconets to detect the frequency channels occupied by the WLAN network and avoid these frequencies in their hopping patterns.

Fig. 8(b) depicts a similar behavior, but with 30% BT traffic load $(\rho_0 = 0.7)$ in each piconet. The presence of idle times within BT packet transmissions causes a more gradual decrease in the CSMA's channel throughput compared with the saturated case. It is interesting to observe here that it takes approximately $2N$ number of BT piconets with 30% traffic load to generate the same degradation as N number of piconets with 100% traffic load. In other words, for a given WLAN channel throughput with saturated BT interferers, we can afford twice the number of BT piconets if they reduce their traffic load by 70%.

Furthermore, we add that the small difference in the numerical and simulation results is due to the assumption of i.i.d. BT interference for each CSMA packet, which was considered in the analysis but relaxed in the simulation modeling.

Fig. 9 plots the CSMA throughput as a function of the offered traffic load $G = g \cdot M \cdot T_{W,N}$ for different values of

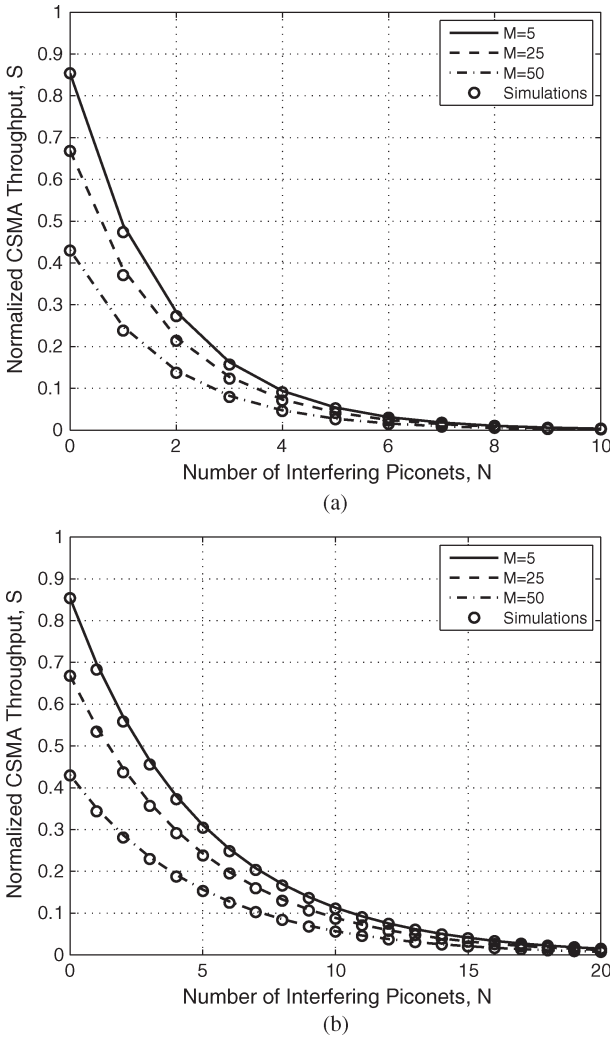

Fig. 8. CSMA throughput as a function of the number of collocated BT piconets N, WLAN packet size $= 1400$ B ($T_W = 1193$ μs), $g = 0.1$, and $p = 0.03$. (a) 100% BT traffic load. (b) 30% BT traffic load. M is the total number of CSMA users.

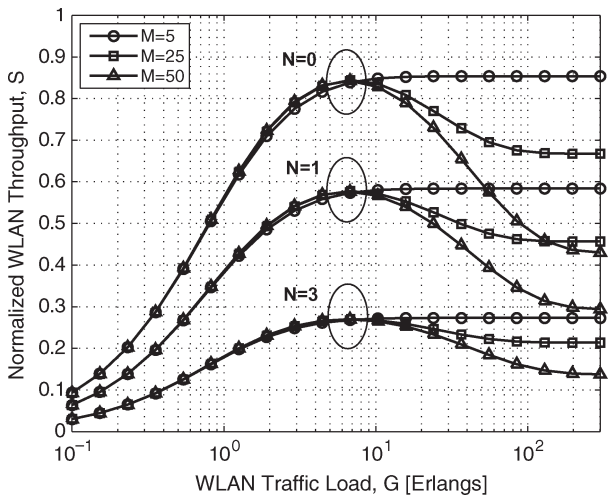

Fig. 9. CSMA throughput as a function of its offered traffic load G, WLAN packet size $= 1400$ B ($T_W = 1193$ μs), $p = 0.03$, 60% BT piconet traffic ($\rho_0 = 0.4$), and equal arrivals of DH1/3/5 ($\rho_1 = \rho_3 = \rho_5$).

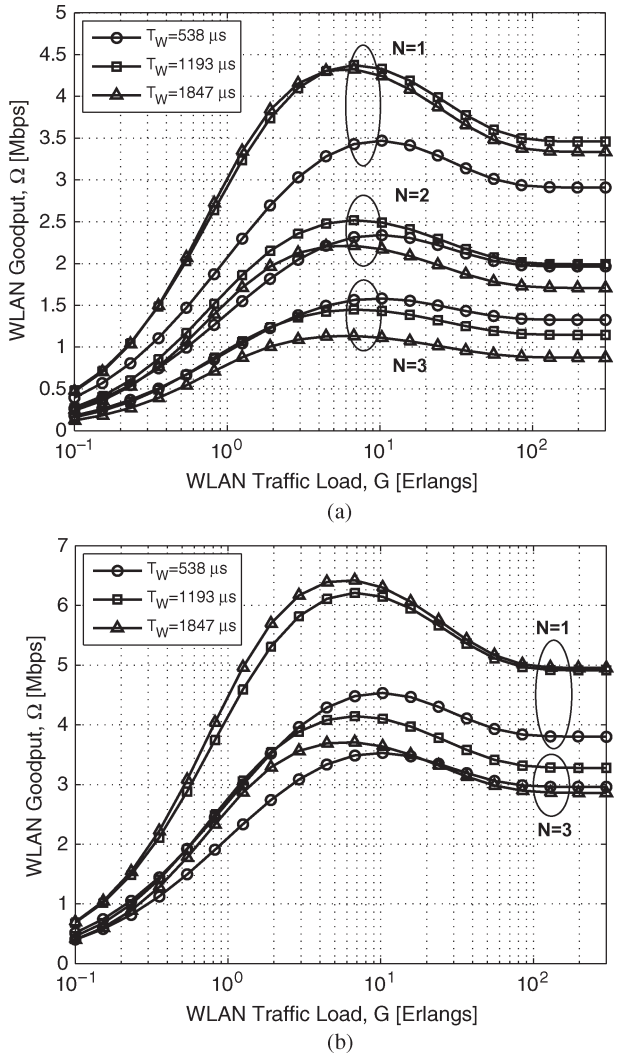

Fig. 10. WLAN goodput as a function of its offered traffic load G, $M = 25$, and $p = 0.03$. (a) 100% BT traffic load. (b) 30% BT traffic load. Equal arrivals of DH1/3/5 are considered ($\rho_1 = \rho_3 = \rho_5$).

its contending users M and number of interfering piconets N. For sake of clarity, the simulation results are not plotted. The graph illustrates that the presence of interfering BT piconets limits the peak CSMA throughput compared with the $N = 0$ case. Furthermore, it can again be observed that the presence of heterogeneous networks is much more catastrophic to the channel throughput than a considerable increase in the number of homogenous terminals and/or homogeneous traffic load. The graph also draws the conclusion that the effect of a higher number of BT piconets is uniform across all values of G and M.

Next, we focus on the goodput performance of the CSMA protocol under cochannel interference. From Fig. 2, the total PHY and MAC overhead can be calculated as $T_{\rm OH} = 216.73$ μs. Therefore, the CSMA goodput, which is denoted by Ω, is given as

$$\Omega = 11 \cdot S \cdot \left(\frac{T_W - T_{\rm OH}}{T_W} \right) \qquad \text{(in megabits per second)} \quad (8)$$

where S is calculated from (5).

Fig. 10 plots the WLAN goodput Ω as a function of its traffic load G and different packet lengths T_W. Fig. 10(a)

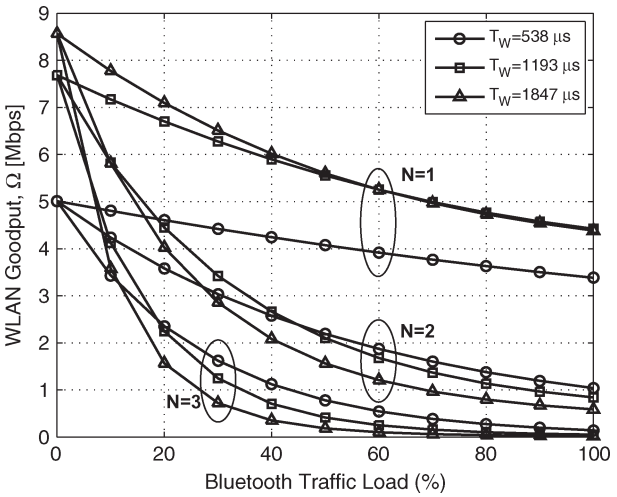

Fig. 11. WLAN goodput as a function of traffic load in each BT piconet: $M = 5$, $p = 0.03$, $g = 0.1$, and equal arrivals of DH1/3/5 ($\rho_1 = \rho_3 = \rho_5$).

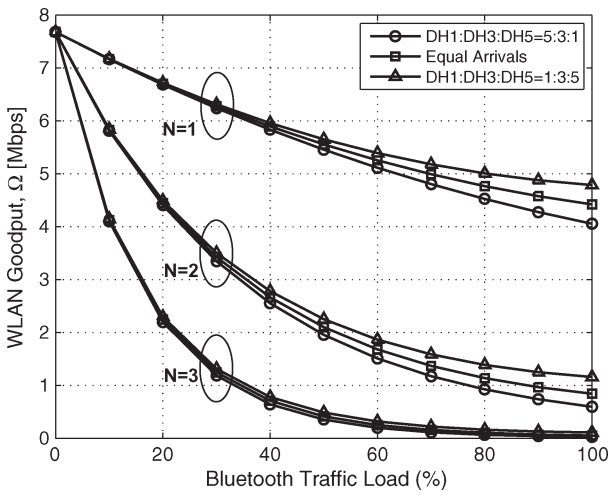

Fig. 12. WLAN goodput as a function of traffic load in each BT piconet: $M = 5$, $p = 0.03$, $g = 0.1$, WLAN packet size = 1400 B ($T_W = 1193$ μs), and different arrivals of DH1/3/5.

shows the results for 100% traffic in each BT piconet, whereas Fig. 10(b) depicts the performance for 30% traffic in each piconet. The plots illustrate that, given a certain BT traffic load and low levels of BT interference (e.g., $N = 1$), it is generally advantageous to transmit longer WLAN packets to achieve a higher goodput across all values of G. However, for greater BT interference ($N = 2$ or 3) at a fixed BT traffic load, there exists an optimal WLAN packet size for a given value of G. Furthermore, at excessive BT interference levels, the plots advocate the transmission of shorter WLAN packets to achieve higher goodput values. This is due to the higher success probability $P_{\rm BT}^S$ for shorter packet durations of WLAN.

In contrast with Fig. 10, Fig. 11 investigates optimal CSMA packet transmission strategies in dependency of the traffic load in each interfering BT piconet. We observe that the choice of a packet size in WLAN to achieve the maximum throughput is strongly dependent on the traffic loads in the interfering BT piconets. Generally, at low BT traffic loads, longer WLAN packets yield higher goodput values, whereas curves for shorter WLAN packets ($T_W = 538$ μs) cross over their longer counter parts and perform better at higher BT traffic loads. However, the cutoff point where this switch takes place is different for different number of piconets N. As an example, for $N = 2$, $T_W = 538$ μs achieves the highest goodput for BT traffic load $> 45\%$ ($\rho_0 \leq 0.55$), whereas for $N = 3$, $T_W = 538$ μs performs better than other packet lengths for BT traffic loads $> 20\%$ ($\rho_0 \leq 0.8$).

In Fig. 12, we observe the effect of different packet arrival models in each BT piconet on the goodput performance of p-persistent CSMA. The plot shows that a higher proportion of shorter packets (e.g., DH1) in BT traffic causes more interference and CSMA goodput degradation. This is because shorter DH1 packets result in a higher probability of collision to a WLAN packet. However, this effect is not visible for low BT traffic loads, where all three BT packet arrival models pose similar interference patterns. Furthermore, we observe that in the presence of a high number of interfering piconets $N = 3$, the different BT packet arrival models pose the same CSMA goodput performance.

The results in Figs. 10–12 draw the conclusion that in the presence of BT interference and for a given number of users M, the maximum WLAN goodput Ω can be achieved by optimizing the WLAN packet size as a function of the interfering BT piconet traffic load, the packet arrival models in BT piconets, and its own traffic load G. From a pragmatic point of view, this is only possible if some means of cooperation exist between the two systems so that WLAN can import BT traffic information and use it to optimize its packet sizes.

V. Carrier-Sense Multiple-Access/ Collision-Avoidance Delay Performance

To calculate the CSMA/CA delay performance, we follow the methodology proposed by Gkelias *et al.* in [41]. Specifically, the model in [41] calculates the average end-to-end packet delay in a p-persistent CSMA/CA network taking into account packet collisions within the CSMA nodes only. By integrating the already derived $P_{\rm BT}^S$ into the framework, we analyze the effect of BT interference on CSMA packet delay characteristics.

Using the p-persistent CSMA model shown in Fig. 7 and the same notational descriptions as per [39] and [41], the unconditional probability of successful transmission for a specific user in the absence of any intersystem BT interference has been derived in [41] and is given as

$$P_s^{(j)} = \frac{p}{1-(1-g)^{XM}} \sum_{k=0}^{\infty} \times \left\{ (1-p)^k - (1-g)^X \left[\frac{p(1-p)^k - g(1-g)^k}{p-g} \right] \right\} \cdot \left\{ (1-p)^{k+1} - p(1-g)^X \times \left[\frac{(1-p)^{k+1} - (1-g)^{k+1}}{p-g} \right] \right\}^{M-1} - \frac{pg(1-g)^{XM}}{1-(1-g)^{XM}} \sum_{k=1}^{\infty} \left[\frac{(1-g)^k - (1-p)^k}{p-g} \right] \cdot \left[\frac{p(1-g)^{k+1} - g(1-p)^{k+1}}{p-g} \right]^{M-1} \tag{9}$$

(10)

where $X = 1$ slot for $j = 1$, and $X = (T_{W,N})$ slots for $j \geq 2$. To incorporate the BT interference, we denote the probability of CSMA packet to be successful in the presence of both intrasystem (due to channel contention between CSMA users) and intersystem (due to time and frequency overlapping of BT packets) interference by $\breve{P}_s$. Thus

$$\breve{P}_s^{(j)} = P_s^{(j)} \cdot P_{\mathrm{BT}}^{S}. \tag{11}$$

Equation (11) gives the probability of a CSMA terminal both generating and successfully transmitting a packet in the jth sub(busy)period.

The probability of failure for a specific terminal in the jth sub(busy)period, given that the terminal has generated a packet, is given by $P_f^{(j)} = 1 - \breve{P}_s^{(j)}/1 - P_e^{(j)}$, where $P_e^{(j)}$ is the probability of a specific user not having any packet arrivals during the jth sub(busy)period and is given by [41]

$$P_e^{(j)} = \frac{1-(1-g)^{X(M-1)}}{1-(1-g)^{XM}}(1-g)^{\left(X+\frac{\overline{D^{(j)}}}{a}\right)}. \tag{12}$$

Therefore, by considering external BT interference, the corresponding probability of failure in the first attempt to access the channel is rewritten as

$$P_f = \frac{\bar{I}+\overline{D^{(1)}}}{\bar{I}+\bar{B}}\left[1-\frac{\breve{P}_s^{(1)}}{1-P_e^{(1)}}\right] + \frac{\bar{B}-\overline{D^{(1)}}}{\bar{I}+\bar{B}}\left[1-\frac{\breve{P}_s^{(2)}}{1-P_e^{(2)}}\right] \tag{13}$$

where the average delay in the jth sub(busy)period is given as [39]

$$\begin{aligned}\overline{D^{(j)}} = {} & \frac{a}{1-(1-g)^{XM}}\sum_{k=1}^{\infty} \\ & \times\left\{(1-p)^k-(1-g)^X p\left[\frac{(1-p)^k-(1-g)^k}{p-g}\right]\right\}^M \\ & -\frac{a(1-g)^{XM}}{1-(1-g)^{XM}}\sum_{k=1}^{\infty}\left[\frac{p(1-g)^k-g(1-p)^k}{p-g}\right]^M.\end{aligned} \tag{14}$$

As in [41], the expected normalized (to the packet length) end-to-end delay from the time a user senses the channel after generating a packet to the end of its successful transmission is given by $\overline{D_{\mathrm{end}}} = 1/T_W \cdot (\bar{L} + \overline{D_r} + T_W)$, where the equation for $\bar{L}$ has been duly formulated therein. For the case of integrating BT interference, the expected normalized delay due to retransmissions is given by

$$\overline{D_r} = \frac{P_f}{\bar{J}\breve{P}_s^{(1)}}\left(T_W + \bar{I} + \overline{D^{(1)}}\right) + \frac{(\bar{J}-1)P_f}{\bar{J}\breve{P}_s^{(2)}}\left(T_W + \overline{D^{(2)}}\right). \tag{15}$$

A. Numerical Results

In this section, the results for the derived normalized delay are presented. The setup for analytical and simulation results is exactly the same as described in Section IV-A.

Fig. 13 depicts the delay performance of p-persistent CSMA in the presence of N number of interfering BT piconets.

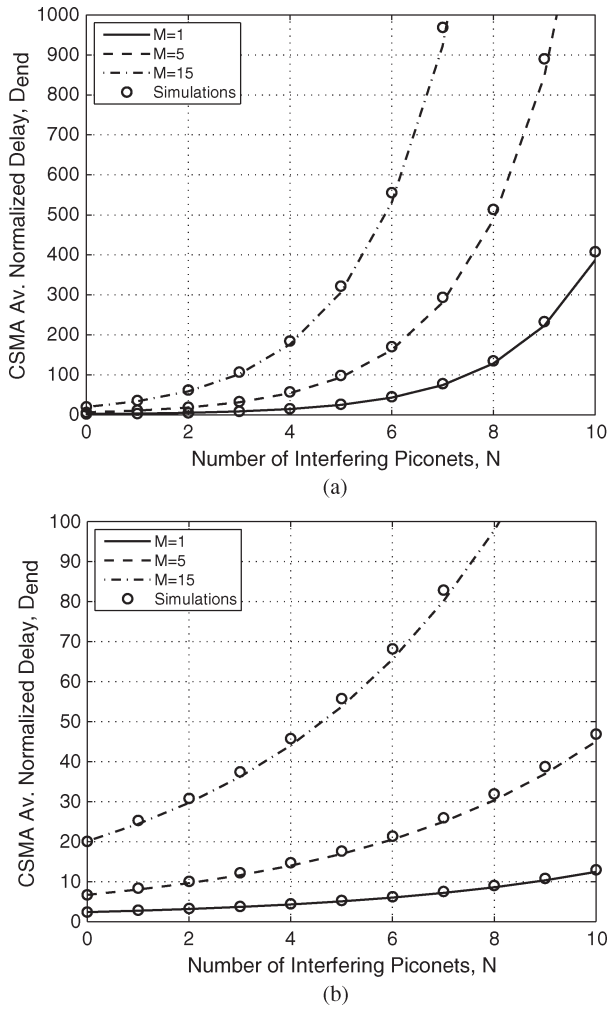

Fig. 13. Average end-to-end CSMA delay as a function of the number of collocated BT piconets N, WLAN packet size = 1400 B ($T_W = 1193$ μs), $g = 0.1$, and $p = 0.03$. (a) 100% BT traffic load. (b) 30% BT traffic load. M is the total number of CSMA users.

Fig. 13(a) and (b) has been plotted for 100% and 30% traffic load per piconet, respectively. The plots give a quantitative *overview* of the effect of BT interference on the end-to-end packet delay of p-persistent CSMA networks. More specifically, they show that, first, the CSMA's end-to-end delay increases with an increasing number of BT networks, and second, the interference effect becomes more pronounced with higher traffic in the piconets ($\rho_0 = 0$). For the same number of piconets, the expected CSMA packet delay is approximately ten times greater for 100% piconet traffic, as compared with the 30% traffic case.

A more detailed investigation of these two graphs shows that, in Fig. 13(a), the normalized delay is increased by a factor of approximately 1.7 (or 70%) for each interfering BT piconet with 100% traffic load. This factor is the same for different number of WLAN terminals. It can be observed that the WLAN system becomes impractical for delay-critical applications in the presence of even one fully loaded BT piconet (e.g., for a network of $M = 5$ WLAN terminals, the normalized delay has a value of $D_{\mathrm{end}} \approx 11$ in the presence of $N = 1$ BT piconet with 100% traffic load). However, if the BT piconets are lightly

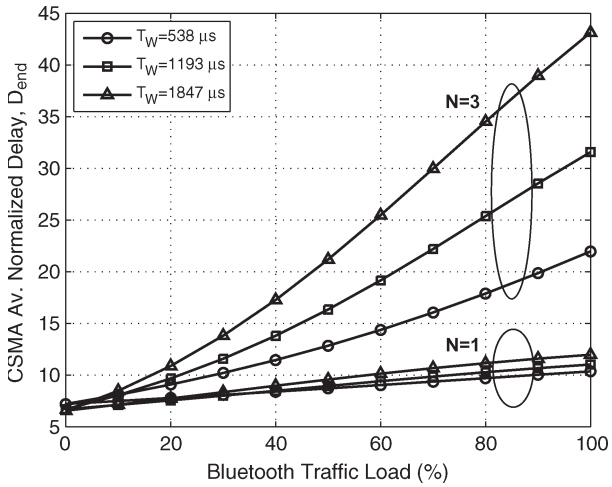

Fig. 14. Average end-to-end CSMA delay as a function of traffic load in each BT piconet: $M = 5$, $p = 0.03$, $g = 0.1$, and equal arrivals of DH1/3/5 ($\rho_1 = \rho_3 = \rho_5$).

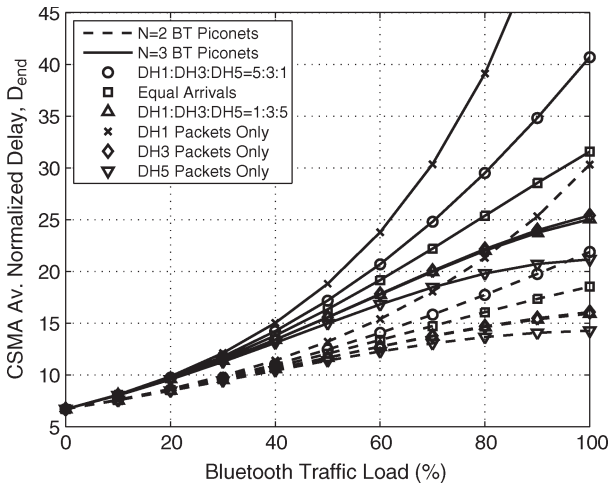

Fig. 15. Average end-to-end CSMA delay as a function of traffic load in each BT piconet: $M = 5$, $p = 0.03$, and $g = 0.1$, WLAN packet size = 1400 B ($T_W = 1193$ μs), and different arrivals of DH1/3/5.

loaded, as can be observed in Fig. 13(b), where 30% BT traffic load is considered, the normalized delay is increased only by a factor of 1.2 (or 20%) per interfering BT piconet. In this case, $N \approx 3$ BT piconets are needed to increase the normalized delay to the same value as in the aforementioned scenario of $M = 5$ WLAN terminals.

In Fig. 14, we study the WLAN packet delay characteristics as a function of different packet sizes. The graph shows that the WLAN delay D_{end} is expectedly higher for longer packet lengths for a certain data traffic in BT piconets. The difference in D_{end} for various packet lengths gets aggravated for higher BT traffic load and higher number of BT piconets. This shows that the choice of WLAN packet size becomes critically important for delay-sensitive applications in the presence of a large number of interfering BT piconets.

It is interesting, however, to compare the results computed in Fig. 14 with those from Fig. 11, where the WLAN goodput Ω is depicted. As earlier stated, for the marginal case of only one BT piconet, i.e., $N = 1$, longer WLAN packets suffer from higher delay, albeit the increase is trivial. On the other hand, as observed in Fig. 11, long and medium WLAN packet sizes can give around 20% higher goodput, as compared with shorter packets. However, as the number of interfering piconet increases, i.e., $N = 3$, both WLAN goodput and normalized packet delay are affected in a similar way (particularly when the BT load is greater than 20%), and shorter WLAN packets appear to give better performance. Therefore, it is preferable to use longer WLAN packets in the case of a single BT interfering piconet and shorter WLAN packets as the number of interfering piconets increases.

Fig. 15 investigates the CSMA packet delay behavior for different packet arrival models in interfering BT piconets. The plot highlights that a higher ratio of smaller packets in BT traffic (DH1 or DH3) results in increased packet delays in CSMA due to a higher probability of collision. Under fully loaded BT traffic conditions, $N = 2$ BT piconets only transmitting single-slot DH1 packets cause higher CSMA delays compared with $N = 3$ BT piconets transmitting a higher proportion of longer packets (DH1 : DH3 : DH5 $= 1 : 3 : 5$). Furthermore, the case of DH1 : DH3 : DH5 $= 1 : 3 : 5$ causes the same WLAN performance as if only DH3 packets were transmitted, which means that the effects of using short and long BT packets are canceled out if their ratio is DH1 : DH5 $= 1 : 5$. Therefore, longer BT packets should be preferable in such heterogeneous interference environments (both for WLAN and BT performance [9]). However, for the decision of optimum BT packet size, the channel conditions must also be taken into account [42], since longer packets are more vulnerable to bit errors. On the other hand, there are many BT applications with small and bursty traffic loads where single-slot packets must inevitably be used, and thus, there is little or no room to design optimal packet strategies.

VI. Conclusion

Passive coexistence is a term used to define the scenario when the collocated PRNs practice no special measures to mitigate or cancel the mutual interference but instead simply operate as they would in an interference-free environment [32]. In such conditions, technologies like BT, which employ FHSS, provide some resistance against the interference by constantly hopping to a new frequency channel. However, networks such as IEEE-802.11-based WLANs, which generally use the same frequency channel, are more prone to a constant source of interference.

The work presented in this paper has provided insights into the passive coexistence behavior of a p-persistent CSMA-based WLAN, where the performance of a CSMA-based WLAN has been shown to be severely degraded in the presence of a number of interfering BT piconets. In particular, the throughput and delay characteristics of the interfered CSMA-based WLAN have been analyzed, and results showed that an increase in BT piconet population causes an exponential decrease in the performance of the p-persistent CSMA system. Specifically, for a certain set of CSMA parameters ($M = 5$, $p = 0.03$, and $g = 0.1$), a 42% reduction in its throughput can be observed in the presence of just one fully loaded BT piconet. Furthermore, WLAN has been shown to have a higher packet latency profile

for more shorter packets in BT traffic, as opposed to a higher number of interfering BT piconets, but transmitting more longer packet sizes.

Finally, while applied to specific WLAN and BT settings, our theoretical analysis facilitates a framework to aid in the design of future heterogeneous networks in unlicensed spectrum. As an example, the derived formulas can be used to optimize the WLAN packet sizes for delay-critical applications in the presence of BT interference. Moreover, the analysis indicates that the complexity of the heterogeneous interference environment (owing to a large number of parameters) demands some level of intersystem collaboration to achieve high performance in the victim network. One such form of cooperation can be the notification to the victim network of the traffic characteristics in the interfering network, and based on this, optimized scheduling patterns or packet fragmentation policies can be designed.

REFERENCES

[1] J. M. Peha, "Wireless communications and coexistence for smart environments," *IEEE Pers. Commun.*, vol. 7, no. 5, pp. 66–68, Oct. 2000.

[2] F. Florén, A. Stranne, O. Edfors, and B.-A. Molin, "Throughput of strongly interfering slow frequency-hopping networks," *IEEE Trans. Commun.*, vol. 52, no. 7, pp. 1152–1159, Jul. 2004.

[3] I. Howitt, "WLAN and WPAN coexistence in UL band," *IEEE Trans. Veh. Technol.*, vol. 50, no. 4, pp. 1114–1124, Jul. 2001.

[4] T.-Y. Lin, Y.-K. Liu, and Y.-C. Tseng, "An improved packet collision analysis for multi-Bluetooth piconets considering frequency-hopping guard time effect," *IEEE J. Sel. Areas Commun.*, vol. 22, no. 10, pp. 2087–2094, Dec. 2004.

[5] S. M. Mishra, S. Ten Brink, R. Mahadevappa, and R. W. Brodersen, "Detect and avoid: An ultra-wideband/WiMAX coexistence mechanism," *IEEE Commun. Mag.*, vol. 45, no. 6, pp. 68–75, Jun. 2007.

[6] I. Howitt and A. Shukla, "Coexistence empirical study and analytical model for low-rate WPAN and IEEE 802.11b," in *Proc. IEEE WCNC*, Las Vegas, NV, 2008, pp. 900–905.

[7] S. Y. Shin, H. S. Park, S. Choi, and W. H. Kwon, "Packet error rate analysis of ZigBee under WLAN and Bluetooth interferences," *IEEE Trans. Wireless Commun.*, vol. 6, no. 8, pp. 2825–2830, Aug. 2007.

[8] R. J. Punnoose, R. S. Tseng, and D. Stancil, "Experimental results for interference between Bluetooth and IEEE 802.11b DSSS systems," in *Proc. IEEE VTC*, Atlantic City, NJ, Oct. 2001, pp. 67–71.

[9] I. Ashraf, A. Gkelias, K. Voulgaris, M. Dohler, and A. H. Aghvami, "Coexistence of CSMA/CA and Bluetooth," in *Proc. IEEE ICC*, Istanbul, Turkey, Jun. 2006, pp. 5522–5527.

[10] J. Lansford, A. Stephens, and R. Nevo, "Wi-Fi (802.11b) and Bluetooth: Enabling coexistence," *IEEE Netw.*, vol. 15, no. 5, pp. 20–27, Sep./Oct. 2001.

[11] C. F. Chiasserini and R. R. Rao, "Co-existence mechanisms for interference mitigation in the 2.4 GHz ISM band," *IEEE Trans. Wireless Commun.*, vol. 2, no. 5, pp. 964–975, Sep. 2003.

[12] I. Howitt, "Bluetooth performance in the presence of 802.11b WLAN," *IEEE Trans. Veh. Technol.*, vol. 51, no. 6, pp. 1640–1651, Nov. 2002.

[13] A. Conti, D. Dardari, G. Pasolini, and O. Andrisano, "Bluetooth and IEEE 802.11b coexistence: Analytical performance evaluation in fading channels," *IEEE J. Sel. Areas Commun.*, vol. 21, no. 2, pp. 259–269, Feb. 2003.

[14] A. Stranne, O. Edfors, and B.-A. Molin, "Energy-based interference analysis of heterogeneous packet radio networks," *IEEE Trans. Commun.*, vol. 54, no. 7, pp. 1299–1309, Jul. 2006.

[15] F. A. Tobagi, "Interactions between the physical layer and upper layers in wireless networks: The devil is in the details," in *Proc. 3rd Int. Conf. BROADNETS*, San José, CA, Oct. 2006.

[16] R. Etkin, A. Parekh, and D. Tse, "Spectrum sharing in unlicensed bands," *IEEE J. Sel. Areas Commun.*, vol. 25, no. 3, pp. 517–528, Apr. 2007.

[17] E. Ferro and F. Potori, "Bluetooth and Wi-Fi wireless protocols: A survey and a comparison," *Wireless Commun.*, vol. 12, no. 1, pp. 12–26, Feb. 2005.

[18] A. Soltanian and R. E. Van Dyck, "Physical layer performance for coexistence of Bluetooth and IEEE 802.11b," in *Proc. Virginia Tech Symp. Wireless Pers. Commun.*, Blacksburg, VA, Jun. 2001.

[19] K. Matheus and S. Zürbes, "Co-existence of Bluetooth and IEEE 802.1b WLANs: Results from a radio network testbed," in *Proc. IEEE PIMRC*, Lisbon, Portugal, Sep. 2002.

[20] K. Matheus and S. Magnusson, "Bluetooth radio network performance: Measurement results and simulation models," in *Proc. Int. Workshop Wireless Ad-Hoc Netw.*, Oulu, Finland, Jun. 2004, pp. 228–232.

[21] N. Golmie and F. Mouveaux, "Interference in the 2.4 GHz ISM band: Impact on the Bluetooth access control performance," in *Proc. IEEE ICC*, Helsinki, Finland, Jun. 2001, pp. 2540–2545.

[22] N. Golmie, R. E. Van Dyck, and A. Soltanian, "Interference of Bluetooth and IEEE 802.11: Simulation modeling and performance evaluation," in *Proc. 4th ACM Int. Workshop Model., Anal. Simul. Wireless Mobile Syst.*, Rome, Italy, Jul. 2001, pp. 11–18.

[23] N. Golmie, R. E. Van Dyck, A. Soltanian, A. Tonnerre, and O. Rébala, "Interference evaluation of Bluetooth and IEEE 802.11b systems," *Wirel. Netw.*, vol. 9, no. 3, pp. 201–211, May 2003.

[24] L. Ophir, Y. Bitran, and I. Sherman, "Wi-Fi (IEEE 802.11) and Bluetooth coexistence: Issues and solutions," in *Proc. IEEE PIMRC*, Barcelona, Spain, Sep. 2004, pp. 847–852.

[25] C. F. Chiasserini and R. R. Rao, "Coexistence mechanisms for interference mitigation between IEEE 802.11 WLANs and Bluetooth," in *Proc. IEEE INFOCOM*, New York, Jun. 2002, pp. 590–598.

[26] I. Ashraf, A. Gkelias, M. Dohler, and A. H. Aghvami, "Time-synchronized multi-piconet Bluetooth environments," *Proc. Inst. Elect. Eng.—Commun.*, vol. 153, no. 3, pp. 445–452, Jun. 2006.

[27] R. Bruno, M. Conti, and E. Gregori, "Optimal capacity of p-persistent CSMA protocols," *IEEE Commun. Lett.*, vol. 7, no. 3, pp. 139–141, Mar. 2003.

[28] F. Calì, M. Conti, and E. Gregori, "IEEE 802.11 protocol: Design and performance evaluation of an adaptive backoff mechanism," *IEEE J. Sel. Areas Commun.*, vol. 18, no. 9, pp. 1774–1786, Sep. 2000.

[29] F. Calì, M. Conti, and E. Gregori, "Dynamic tuning of the IEEE 802.11 protocol to achieve a theoretical throughput limit," *IEEE/ACM Trans. Netw.*, vol. 8, no. 6, pp. 785–799, Dec. 2000.

[30] J. H. Kim and J. K. Lee, "Capture effects of wireless CSMA/CA protocols in Rayleigh and shadow fading channels," *IEEE Trans. Veh. Technol.*, vol. 48, no. 4, pp. 1277–1286, Jul. 1999.

[31] V. Subramanian, K. K. Ramakrishnan, S. Kalyanaraman, and L. Ji, "Impact of interference and capture effects in 802.11 wireless networks on TCP," in *Proc. 2nd Int. Workshop WitMeMo*, New York, 2006.

[32] R. Morrow, *Wireless Network Coexistence*. New York: McGraw-Hill, 2004.

[33] Part 11: Wireless LAN Medium Access Control (MAC) and Physical (PHY) Specifications, IEEE Std. 802.11b-1999, 1999.

[34] A. El-Hoiydi, "Interference between Bluetooth networks—Upper bound on the packet error rate," *IEEE Commun. Lett.*, vol. 5, no. 6, pp. 245–247, Jun. 2001.

[35] T.-Y. Lin and Y.-C. Tseng, "Collision analysis for a multi-Bluetooth picocells environment," *IEEE Commun. Lett.*, vol. 7, no. 10, pp. 475–477, Oct. 2003.

[36] G. Pasolini, "Analytical investigation on the coexistence of Bluetooth piconets," *IEEE Commun. Lett.*, vol. 8, no. 3, pp. 144–146, Mar. 2004.

[37] B. S. Peterson, R. O. Baldwin, J. P. Kharoufeh, and R. A. Raines, "Refinements to the packet error rate upper bound for Bluetooth networks," *IEEE Commun. Lett.*, vol. 7, no. 8, pp. 284–382, Aug. 2003.

[38] Bluetooth Core Spec. v2.1. [Online]. Available: http://www.bluetooth.com

[39] H. Takagi and L. Kleinrock, "Throughput analysis for persistent CSMA systems," *IEEE Trans. Commun.*, vol. COM-33, no. 7, pp. 627–638, Jul. 1985.

[40] N. Golmie, O. Rébala, and N. Chevrollier, "Bluetooth adaptive frequency hopping and scheduling," in *Proc. MILCOM*, Boston, MA, Oct. 2003, pp. 1138–1142.

[41] A. Gkelias, M. Dohler, V. Friderikos, and A. H. Aghvami, "Average packet delay of CSMA/CA with finite user population," *IEEE Commun. Lett.*, vol. 9, no. 3, pp. 273–275, Mar. 2005.

[42] S. Sarkar, F. Anjum, and R. Guha, "Optimal communication in Bluetooth piconets," *IEEE Trans. Veh. Technol.*, vol. 54, no. 2, pp. 709–721, Mar. 2005.

Imran Ashraf (M'09) received the B.Sc. degree in electrical engineering (major in telecommunications) from the University of Engineering and Technology, Lahore, Pakistan, in 2002 and the M.Sc. degree in mobile and personal communications and the Ph.D. degree in telecommunications from King's College, University of London, London, U.K., in 2003 and 2007, respectively.

From 2003 to 2005, he was with the Core 3 research program of the Mobile Virtual Centre of Excellence, U.K. From 2006 to 2007, he was a Research Associate with the Centre for Telecommunications Research, King's College London, where he contributed to European Union-funded research projects on wireless sensor networks. He is currently with Autonomous Networks and Systems Research, Bell Laboratories, Alcatel-Lucent, Swindon, U.K. His research interests include protocol design and performance analysis of wireless ad hoc and sensor networks, cross-layer issues, efficient scheduling algorithms, and self-organizing behavior in cellular radio networks.

Konstantinos Voulgaris (M'09) received the degree from the University of Patras, Patras, Greece, in 1999, the M.Sc. degree in telecommunications, computers, and human-centered systems from the University of Birmingham, Birmingham, U.K., and the Ph.D. degree in telecommunications from King's College London, London, U.K., in 2009.

In October 2000, he was a Universal Mobile Telecommunications System (UMTS) Systems Engineer with Motorola. Within one year, he received the Motorola Bravo Award and shortly after was promoted to Senior Systems Engineer. From April 2003 to April 2004, he was a Third-Generation Terminal Air Interface Expert with T-Mobile, U.K. In 2008, he was a Summer Intern with Bell Laboratories, Alcatel-Lucent, Swindon, U.K. He is currently a Technical Advisor with Ofcom, London. His research interests include medium-access control protocols for wireless sensor networks and beyond third-generation mobile communication systems.

Athanasios Gkelias (M'09) received the Diploma in electrical and computer engineering from Aristotle University of Thessaloniki, Thessaloniki, Greece, in 2000 and the M.Sc. and Ph.D. degrees in telecommunications from King's College London, London, U.K., in 2001 and 2005, respectively.

He was a Visiting Researcher with Bell Laboratories, Alcatel-Lucent, Swindon, U.K., and with Athens Information Technology, Athens, Greece. Since 2006, he has been a Postdoctoral Researcher with Imperial College London. He has published several technical journal and conference papers and has been a Technical Program Committee member of various conferences. His research interests lie in the area of wireless ad hoc, sensor, and mesh networks, particularly in the performance analysis and design of medium access control and quality-of-service routing protocols and cross-layer issues.

Mischa Dohler (SM'07) received the Diploma in electrical engineering from Dresden University of Technology, Dresden, Germany, in 2000 and the M.Sc. and Ph.D. degrees in telecommunications from King's College London, London, U.K., in 1999 and 2003, respectively.

From September 2003 to June 2005, he was a Lecturer with the Centre for Telecommunications Research, King's College London. From June 2005 to February 2008, he was a Senior Research Expert with the R&D Division, France Telecom, where he worked on cooperative communication systems, cognitive radios, and wireless sensor networks. He is currently a Senior Researcher with CTTC, Parc Mediterrani de la Tecnologia, Castelldefels, Spain. He has published more than 110 technical journal and conference papers at a citation h-index of 17 and citation g-index of 34, is the holder of several patents, has coedited and contributed to several books, and has given numerous international short courses and participated in standardization activities. In the framework of the Mobile VCE, he has pioneered research on distributed cooperative space–time encoded communication systems, dating back to December 1999.

Dr. Dohler has been Technical Program Committee member and cochair of various conferences, such as Technical Chair of the 2008 IEEE International Conference on Personal Indoor and Mobile Radio Communications held in Cannes, France. He is the Editor for numerous IEEE and non-IEEE journals. He has also been a London Technology Network Business Fellow with King's College London, as well as Student Representative of the IEEE United Kingdom and Republic of Ireland Section and member of the Student Activity Committee of IEEE Region 8 (Europe, Africa, Middle-East, and Russia). He has won various competitions in mathematics and physics and participated in the third round of the International Physics Olympics for Germany.

A. Hamid Aghvami (M'87–SM'91–F'05) received the M.Sc. and Ph.D. degrees from King's College, University of London, London, U.K., in 1978 and 1981, respectively.

In 1984, he joined King's College London, where he was promoted to Reader in 1989 and to Professor in telecommunications engineering in 1993 and where he is currently the Director of the Centre for Telecommunications Research. He carries out consulting work on digital radio communications systems for both British and international companies. He was a Visiting Professor with NTT Radio Communication Systems Laboratories in 1990 and a Senior Research Fellow with BT Laboratories from 1998 to 1999. From 1996 to 2002, he was an Executive Advisor to Wireless Facilities Inc., USA. He is the Managing Director of Wireless Multimedia Communications LTD (his own consultancy company). He has published over 400 technical papers and given invited talks all over the world on various aspects of personal and mobile radio communications, as well as having given courses on the subject world wide. He leads an active research team working on numerous mobile and personal communications projects for third- and fourth-generation systems. These projects are supported both by the government and industry.

Prof. Aghvami is a Fellow of the Royal Academy of Engineering and the Institution of Engineering and Technology. He was a member of the Board of Governors of the IEEE Communications Society from 2001 to 2003. He is a Distinguished Lecturer of the IEEE Communications Society and has been member, Chairman, and Vice-Chairman of the technical program and organizing committees of a large number of international conferences. He is also the founder of the International Conference on Personal Indoor and Mobile Radio Communications.